JAAS
Journal of Analytical Atomic Spectrometry

Modeling of argon direct current glow discharges and comparison with experiment: how good is the agreement?†

Invited Lecture

Annemie Bogaerts* and Renaat Gijbels

Department of Chemistry, University of Antwerp, Universiteitsplein 1, B-2610 Wilrijk, Belgium

A set of three-dimensional models was developed for the different plasma species in a glow discharge, and these models were combined, to obtain an overall picture of a direct current glow discharge in argon. Typical results of these models include the electrical current flowing through the discharge as a function of pressure and voltage, the density profiles and flux energy distributions of the plasma species, the potential and electric field distributions in the plasma, information on collision processes, the crater profiles due to sputtering at the cathode and optical emission spectra due to radiative decay of excited atoms. The calculated data were compared with experimental observations to check the validity of the models, and the reliability of both modeling and experimental results is discussed.

Keywords: *Glow discharge; modeling; direct current; argon*

Glow discharges are finding increasing application as analytical sources for mass spectrometry and optical spectrometric techniques.[1,2] For good analytical practice, a clear insight into the glow discharge is desirable. This can be obtained by mathematical modeling or by experimental plasma diagnostics. In earlier work, we developed three-dimensional models to describe the behavior of the different plasma species in a direct current glow discharge in argon.[3–12] A short overview of the models is given here. Typical results of the calculations, which are compared with experimental observations, to test the validity of the models are presented. The reliability of both modeling and experimental work is briefly discussed.

OVERVIEW OF THE MODELS

The different species assumed to be present in the plasma, and described in the models, are the argon gas atoms in thermal equilibrium, uniformly distributed throughout the discharge (Ar^0), electrons (sub-divided into a fast and a slow group: e^-_{fast}, e^-_{slow}), argon ions (Ar^+), fast argon atoms, created by charge transfer and elastic collisions from the argon ions (Ar^0_f), argon atoms in various excited levels including the metastable levels (Ar* and Ar^*_m, respectively), and atoms and ions of the cathode material (*i.e.*, the material to be analyzed, M^0 and M^+). Table 1 presents an overview of the models used to describe these species, together with the references of the papers where detailed information can be found.

Two different kinds of model are employed: fluid approaches and Monte Carlo simulations. A fluid model deals with a given plasma species as a fluid, a group, in equilibrium with the electric field, *i.e.*, the energy gained from the electric field is more or less balanced by the energy lost due to collisions. The species are then generally described with the continuity equations and flux equations, based on diffusion and migration in the electric field. This method is, in principle, rather simple, but it is only an approximation. More specifically, it is not able to describe adequately the behavior of fast plasma particles, which are not in equilibrium with the electric field. The Monte Carlo simulations, on the other hand, cope with the non-equilibrium situation of the plasma species and treat them as separate particles. The particles are followed, one after the other, in successive time steps. During each time step, their trajectories are simulated by Newton's laws, and the occurrence of a collision during that time step, the kind of collision, and the new energy and direction after collision, are determined by random numbers. By following in this statistical way a large number of particles, the glow discharge can be simulated. This method is the most accurate one, because it deals with the particles on the microscopic level. However, in order to reach statistically valid results, a long calculation time is required for slow-moving particles.

Therefore, only fast particles, which are not in equilibrium with the electric field, are described with Monte Carlo simulations (*i.e.*, the fast electrons throughout the whole discharge, the sputtered cathode atoms, which leave the cathode with average energies of 5–10 eV, and the argon ions, fast argon atoms, and cathode ions in the cathode dark space; this is the region adjacent to the cathode, where a strong electric field is present). The slow particles, which can be considered in equilibrium with the electric field, are treated in a fluid model; this is the case for the argon ions and slow electrons, the argon metastable atoms, and the atoms and ions of the cathode material.

The models have previously been applied to various cell geometries, *e.g.*, the standard cell for analyzing flat samples in the VG9000 glow discharge mass spectrometer[9–11] (VG Elemental, Thermo Group), a six-way cross glow discharge cell (to make exact comparison with experimental data possible, see below) with various dimensions[13] and with both flat

Table 1 Overview of the species assumed to be present in the plasma, and the models used to describe these species, together with the references of the papers where these models are explained in detail

Plasma species	Model	Ref.
Fast electrons	Monte Carlo model	3,4,9
Slow electrons	Fluid model	4,9
Argon ions	Fluid model	4,9
Argon ions in CDS	Monte Carlo model	3,5,9
Fast argon atoms in CDS	Monte Carlo model	3,5,9
Argon atoms in various excited levels	Fluid model	6,10,12
Cathode atoms (thermalization process)	Monte Carlo model	7,10
Cathode atoms + ions (diffusion, ionization,…)	Fluid model	8,10
Cathode ions in CDS	Monte Carlo model	8,10

†Presented at the 1998 Winter Conference on Plasma Spectrochemistry, Scottsdale, AZ, USA, January 5–10, 1998.

or pin cathodes,[14] and a Grimm-type glow discharge.[15] The Monte Carlo models are developed completely in three dimensions. Owing to the nearly cylindrical symmetry of the discharge cells, the three-dimensional fluid models could be reduced to two-dimensional calculations (*i.e.*, axial and radial directions). The continuity equations of the charged particles in the fluid models are coupled to Poisson's equation to obtain a self-consistent electric field distribution throughout the plasma. Moreover, the models are all coupled to each other through the interaction processes between the plasma species, and they are solved iteratively until final convergence is reached. More information about these models and about the coupling procedure can be found in refs. 3–12 and 16.

RESULTS OF THE MODELS AND COMPARISON WITH EXPERIMENT

An overview of some typical results will be given, and attention will be paid to comparison with experimental data to test the validity of the models. When pressure and voltage are given, the electrical current follows as a self-consistent result from the model. In Fig. 1(*a*), the calculated electrical current as a function of voltage for three pressures, is illustrated for the VG9000 standard flat cell. The current increases with pressure and voltage, as expected. For comparison, Fig. 1(*b*) presents some experimental current–voltage characteristics, at the same pressures. The qualitative agreement between theory and experiment is reasonable. However, exact quantitative agreement is not yet reached. Indeed, the calculations were performed for a slightly different discharge cell from that used for the measurements (*i.e.*, so-called new *versus* old flat cell of the VG9000 glow discharge mass spectrometer). Also, the pressure cannot, in principle, be measured in the VG9000 glow discharge cells. In order to obtain current–voltage characteristics at specific pressures, the pressure was measured with a thermocouple,[17] but these measured pressures are subject to uncertainties. Moreover, the exact gas temperature in the discharge cell is not known. Therefore, a certain gas temperature had to be assumed in the model. The choice of this gas temperature is not straightforward. Generally, the gas is assumed to be at room temperature. In the literature, however, gas temperatures are reported to be of the order of 900–1400 K in a Grimm-type glow discharge.[18] The latter operates, however, at much higher currents (*i.e.*, 40–80 mA), so that higher temperatures are expected than in the VG9000 glow discharge. Moreover, the VG9000 glow discharge cell is cooled with liquid nitrogen, which further complicates the situation (*i.e.*, low temperatures at the walls, but possibly higher temperatures in the plasma). We assumed a gas temperature of 360 K, since this yielded reasonable values for the electrical current. However, since this value is, actually, a kind of fitting parameter (*i.e.*, chosen in order to obtain realistic values for the current), and since small variations in the gas temperature had a significant effect on the electrical current (*e.g.*, 30% variation in absolute gas temperature yields a change in electrical current of 100%), the quantitative results of the model have to be considered with caution. Nevertheless, the gas temperature assumed in the calculations has a reasonable value, which indicates that the model presents a more or less realistic picture of the glow discharge.

An important quantity that can be calculated with the models is the density profile of the plasma species. Fig. 2 presents the argon ion density profile for the VG9000 glow discharge cell, at 1000 V, 75 Pa and 3 mA. The cathode is situated at $z=0$. The Teflon insulator ring, with an aperture diameter of 2 cm, and the front plate at anode potential, with an aperture diameter of 1 cm, are represented by the black

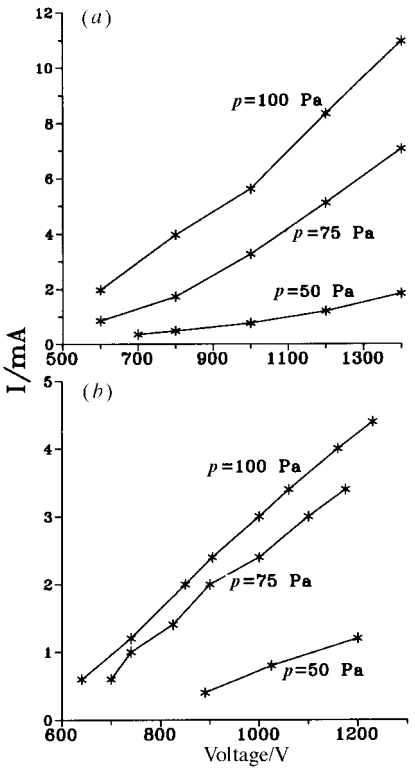

Fig. 1 (*a*) Calculated electrical current as a function of voltage at three pressures (VG9000 glow discharge flat cell, copper cathode in argon). (*b*) Measured electrical current as a function of voltage at three pressures for the VG9000 mass spectrometer (copper cathode in argon).

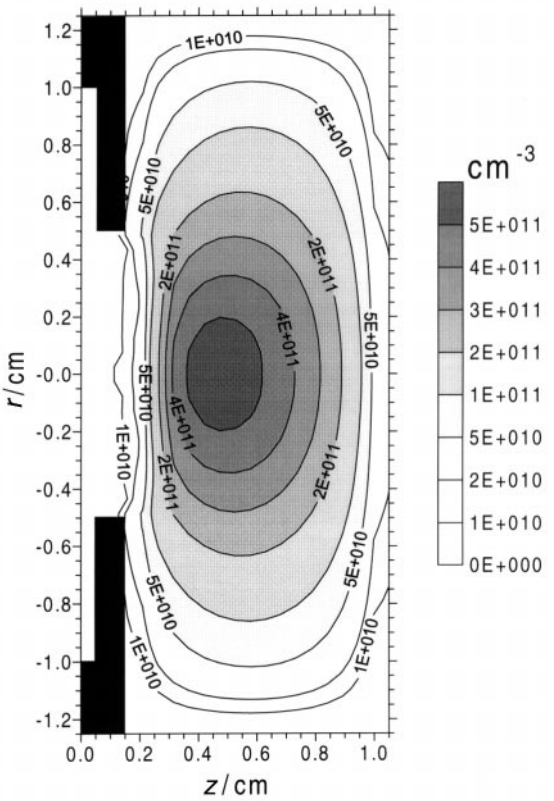

Fig. 2 Calculated density profile of the argon ions throughout the discharge (VG9000 glow discharge flat cell, 75 Pa, 1000 V, 3 mA, copper cathode in argon). Reprinted from ref. 9 with permission of American Chemical Society.

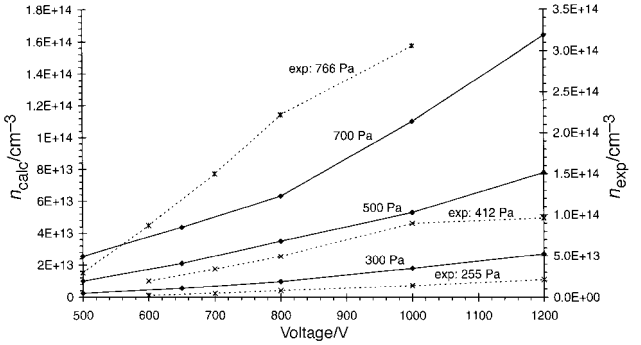

Fig. 3 Calculated densities of the slow electrons (and argon ions) at the maximum of their profiles, as a function of voltage at three pressures (solid lines, left axis), and experimental slow electron densities, measured with Langmuir probe measurements (broken lines, right axis) (Grimm glow discharge cell, copper cathode in argon). Reprinted from ref. 15 with permission of Elsevier Science.

rectangles at $z = 0$–0.5 mm, and at $z = 0.5$–1.5 mm from the cathode, respectively. The anode walls are given by the borders of the figure. The argon ion density is small and relatively constant in the cathode dark space (CDS) and reaches a maximum in the negative glow (NG) (the NG is the region occupying the larger part of the discharge). The slow electron density profile is nearly equal to the argon ion density in the NG, but it is zero in the CDS. This gives rise to a net positive space charge in the CDS and charge neutrality in the NG.

Slow electron densities have been reported in the literature which were obtained by Langmuir probe and by optical emission spectrometry measurements. Our results, calculated for pressures between 50 and 100 Pa (*i.e.*, typical GDMS conditions), are in reasonable agreement with typical values reported for a six-way cross glow discharge (*i.e.*, of the order of 10^{11} cm^{-3}), which operated under similar discharge conditions.[19,20] Moreover, the slow electron densities that we have calculated for a Grimm-type glow discharge under typical GD-OES discharge conditions (*i.e.*, 300–700 Pa, 10–50 mA, 600–1200 V) are about 10^{13}–10^{14} cm^{-3},[15] which is in good agreement with experimental data under comparable discharge conditions,[18,21–23] as is illustrated for example in Fig. 3. The difference between the calculated and experimental (*i.e.*, Langmuir probe) results is only a factor of about 2, which is well below the expected uncertainties of both the modeling work and the Langmuir probe measurements.

In Fig. 4(*a*) the density profile for the argon metastable atoms is shown, for a six-way cross glow discharge cell, at 1000 V, 1 Torr (*i.e.*, 133 Pa) and about 2 mA, calculated with a balance equation consisting of various production and loss processes.[6,10] The cathode is represented by the black line at $z = 0$, whereas the other borders of the figure are the anode walls. The density reaches a pronounced maximum in front of the cathode, and a second, less distinct, maximum at the end of the discharge cell. To check this result of the modeling, the argon metastable atom density profile was measured by laser-induced fluorescence spectroscopy in a similar six-way cross cell and under the same discharge conditions.[24] The resulting density profile is depicted in Fig. 4(*b*). It is also characterized by two distinct maxima. However, the exact positions of the maxima, and also the absolute value of the first maximum, are not yet in complete agreement with the modeling result. This indicates that the model is probably not yet able to describe completely the real situation, in spite of the fact that the model for the metastable atoms is already fairly complicated and exhaustive, *i.e.*, it consists of a balance equation with five different production processes and eight different loss processes (see refs. 6 and 10 for more detailed information). However, the rate coefficients of the different processes are subject to

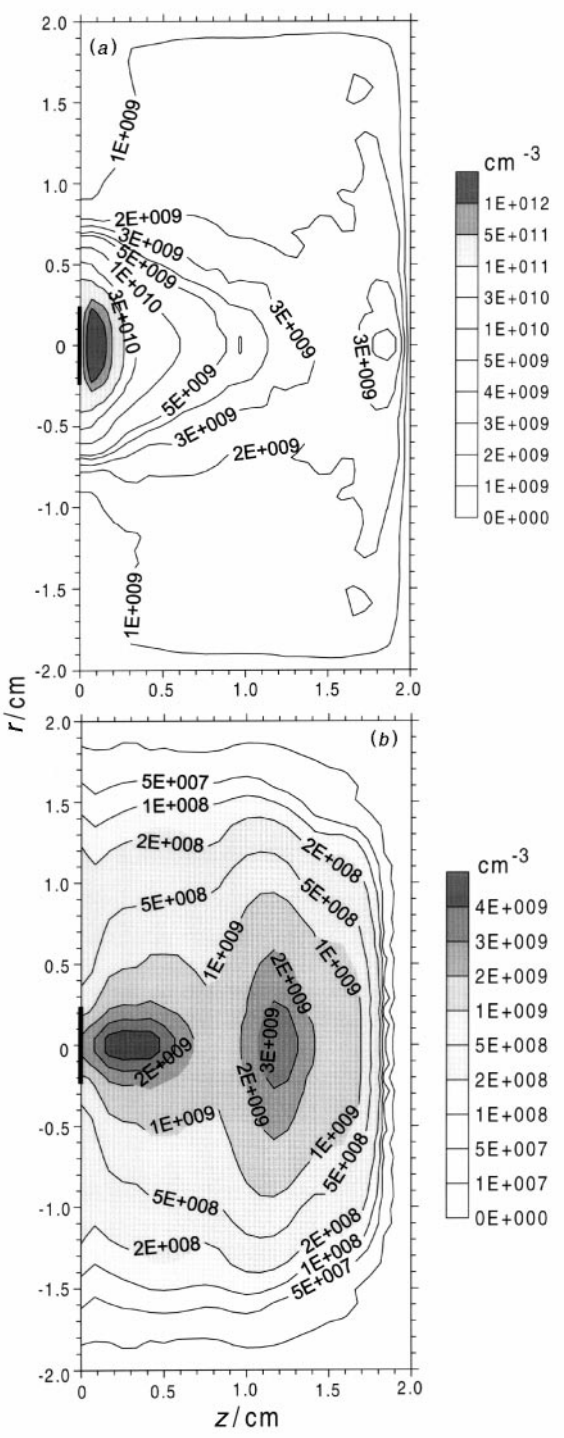

Fig. 4 (*a*) Calculated density profile of the argon metastable atoms throughout the discharge (six-way cross glow discharge cell, 1 Torr, 1000 V, 2 mA, tantalum cathode in argon). (*b*) Experimental density profile of the argon metastable atoms throughout the discharge, measured with laser-induced fluorescence spectroscopy (six-way cross glow discharge cell, 1 Torr, 1000 V, 2 mA, tantalum cathode in argon). Reprinted from ref. 24 with permission of Elsevier Science.

uncertainties and this will have an effect on the resulting calculated density. On the other hand, the experimental profile may also be subject to uncertainties. From the measured laser fluorescence intensity, the absolute density is deduced, but the correctness of this step depends on how well the transition probability of the investigated transition is known and on the reliability of instrument calibrations (electronics, monochromator, photomultiplier tube). Nevertheless, the absolute values of the density profile beyond the pronounced maximum in front

of the cathode are already in satisfactory agreement with the experimental values.

We have recently developed a so-called collisional–radiative model describing the behavior of various excited levels of argon:[12] 64 excited levels or 'level groups' were considered, and a large number of populating and depopulating processes were incorporated, yielding 64 coupled balance equations. In this model, the behavior of the argon metastable levels was also calculated, and in more detail than in the former metastable model which consisted of only one balance equation (*e.g.*, the effect of the other excited levels is now explicitly taken into account). The metastable level density profile calculated with the latter collisional–radiative model for a Grimm-type glow discharge under typical GD-OES discharge conditions is in excellent agreement with metastable density profiles measured by Strauss *et al.*[25] in a Grimm source under similar discharge conditions. This indicates that in spite of the complex and large number of processes that can occur for argon metastable levels, the model is able to present a realistic picture of the behavior of these species.

Fig. 5(*a*) presents the calculated sputtered tantalum atom density profile for the six-way cross glow discharge cell, at 1000 V, 1 Torr and about 2 mA. It reaches a maximum at a few millimetres from the cathode and decreases towards the cell walls. This profile was also compared with experimental results under the same discharge conditions, obtained by laser-induced fluorescence spectroscopy,[26] as is illustrated in Fig. 5(*b*). It can be seen that the theoretical and experimental results are in reasonable agreement, both qualitatively and quantitatively. The tantalum atom density profile was also measured by atomic absorption, and was found to be a factor of 3 lower than the fluorescence result.[26] This illustrates the experimental uncertainty that can be expected (and it may be greater, if the good agreement between the fluorescence and absorption data were only to be coincidence). Hence, it can be concluded that the theoretical and experimental profiles are similar to each other within the experimental error.

The corresponding calculated tantalum ion density profile is given in Fig. 6(*a*), for the six-way cross glow discharge cell, at 1000 V, 1 Torr and about 2 mA. It is fairly constant and low in the CDS and increases to reach a maximum at about 6 mm from the cathode (*i.e.*, in the NG). This density profile is in fairly good qualitative agreement with the experimentally obtained density profile under the same discharge conditions, shown in Fig. 6(*b*).[26] However, exact quantitative agreement is not yet reached, since the calculated density is almost an order of magnitude lower than the experimental result. Since the tantalum atom densities were in satisfactory agreement, this may indicate that the calculated ionization of sputtered tantalum atoms is too low. The ionization processes incorporated in the model are electron impact ionization, Penning ionization by argon metastable atoms and asymmetric charge transfer by argon ions. It is anticipated that the first two ionization processes are correctly described in the model,[26] but the role of asymmetric charge transfer may be underestimated, owing to uncertainties in the rate coefficients. Moreover, it is also possible that other ionization processes come into play, which are neglected in the present model. On the other hand, the experimental density profile is also subject to errors (probably at least a factor of 3, see above), and it is expected that the discrepancy between Fig. 6(*a*) and (*b*) is a combination of some limitations in the model and some experimental errors. After all, the disagreement is not too bad, if one takes into account that these modeling calculations and these experiments have never been performed and confronted before.

Other quantities that can be calculated with the models are the potential and electric field distributions throughout the plasma. The potential distribution for the VG9000 glow discharge cell is presented in Fig. 7, for 1000 V, 75 Pa and about 3 mA. It is −1000 V at the cathode, increases very rapidly in the CDS and goes through zero at 2.4 mm from the cathode. This position is defined by our model as the interface between the CDS and NG. The potential is slightly positive in the NG, and this is called the plasma potential. Fig. 8 shows the calculated length of the CDS as a function of voltage and pressure. It increases slightly with decreasing voltage and more clearly with decreasing pressure. We evaluated these calculated

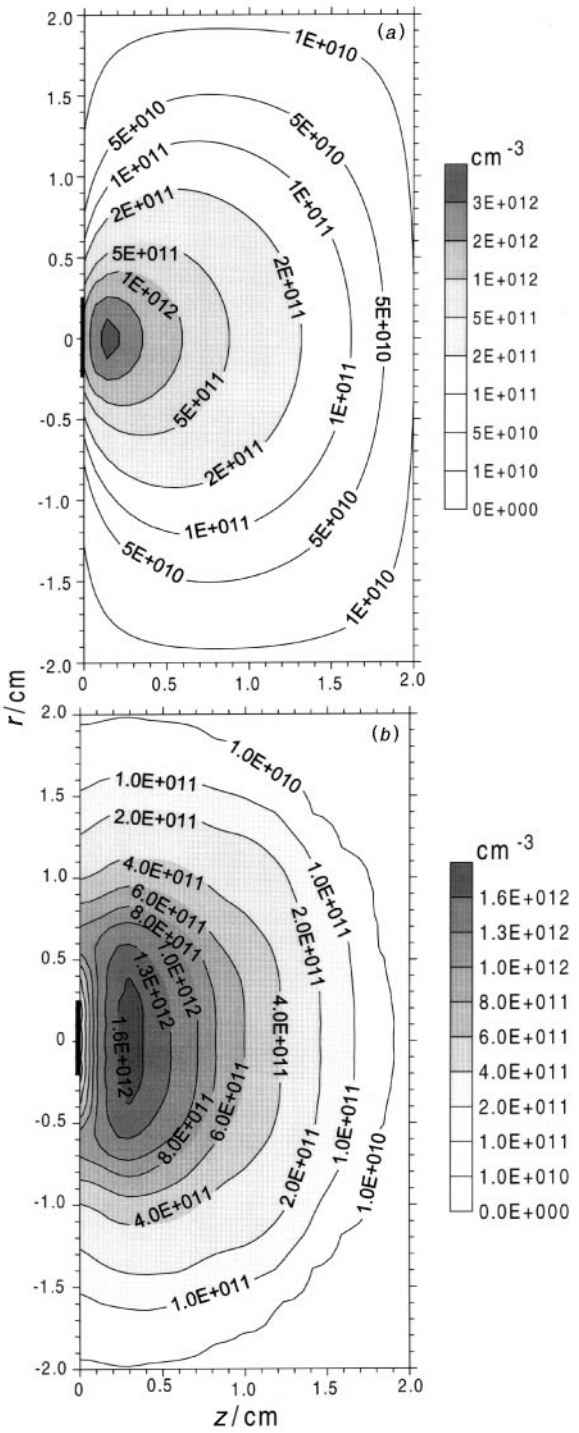

Fig. 5 (*a*) Calculated density profile of the sputtered tantalum atoms throughout the discharge (six-way cross glow discharge cell, 1 Torr, 1000 V, 2 mA, tantalum cathode in argon). (*b*) Experimental density profile of the sputtered tantalum atoms throughout the discharge, measured with laser-induced fluorescence spectroscopy (six-way cross glow discharge cell, 1 Torr, 1000 V, 2 mA, tantalum cathode in argon). Reprinted from ref. 26 with permission of Elsevier Science.

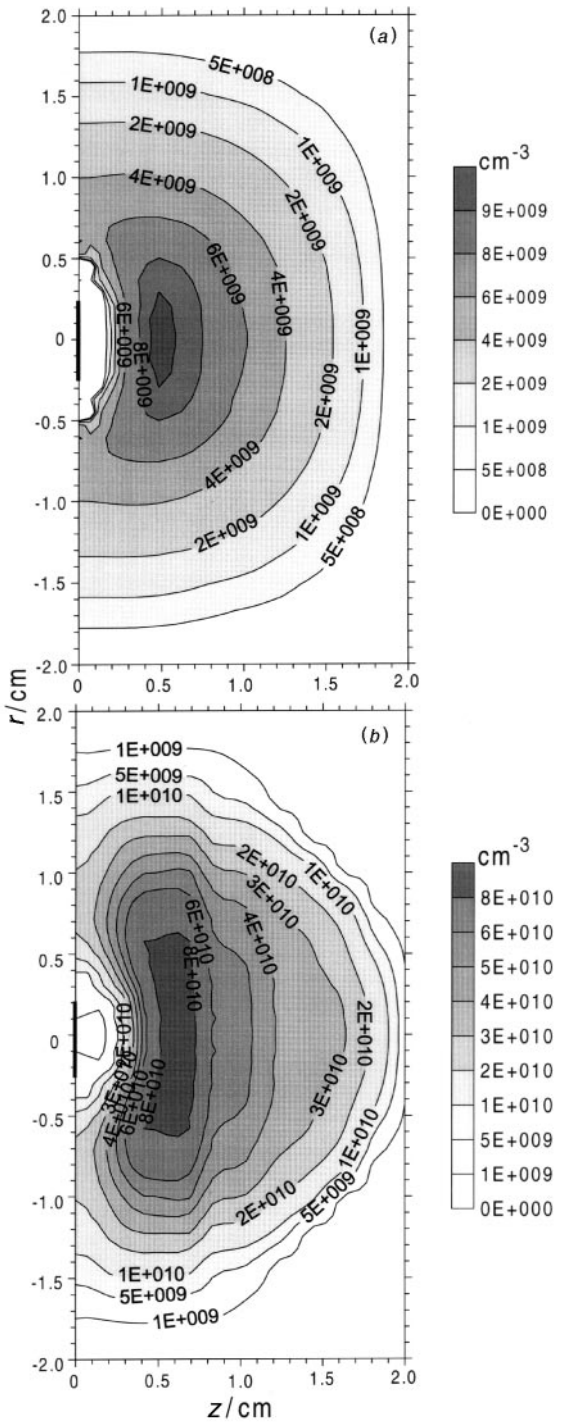

Fig. 6 (*a*) Calculated density profile of the tantalum ions throughout the discharge (six-way cross glow discharge cell, 1 Torr, 1000 V, 2 mA, tantalum cathode in argon). (*b*) Experimental density profile of the tantalum ions throughout the discharge, measured with laser induced fluorescence spectroscopy (six-way cross glow discharge cell, 1 Torr, 1000 V, 2 mA, tantalum cathode in argon). Reprinted from ref. 26 with permission of Elsevier Science.

lengths of the CDS with an empirical relationship, proposed by Aston, between the length of the CDS, d_{CDS}, and pressure and current in the discharge:[27]

$$d_{CDS} = \frac{A}{p} + \frac{B}{I^{1/2}}$$

where A and B are constants. It was indeed found that there is a linear relationship between the calculated d_{CDS} and $I^{1/2}$ at constant pressure.[5,11] The inverse proportionality between d_{CDS}

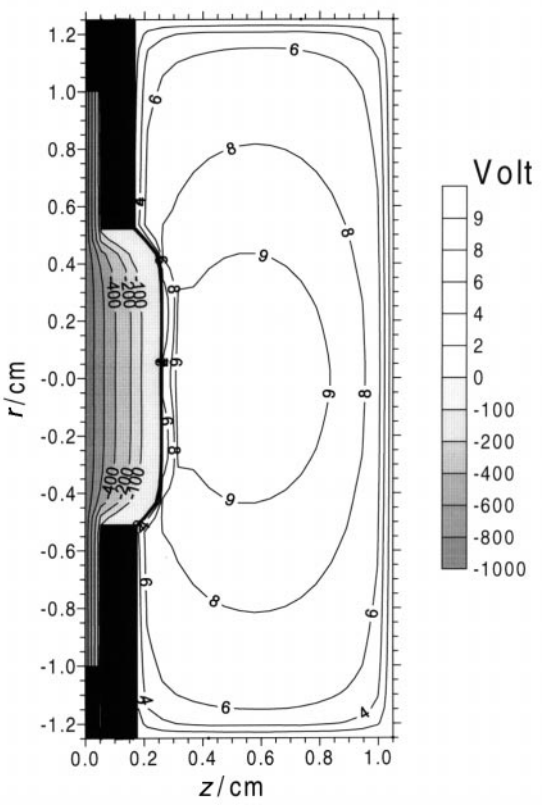

Fig. 7 Calculated potential distribution throughout the discharge (VG9000 glow discharge flat cell, 75 Pa, 1000 V, 3 mA, copper cathode in argon). Reprinted from ref. 9 with permission of American Chemical Society.

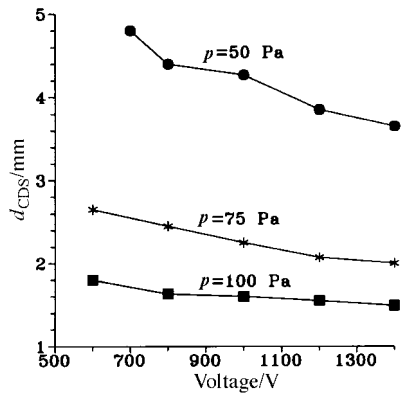

Fig. 8 Calculated length of the cathode dark space (d_{CDS}) as a function of voltage, at three pressures (VG9000 glow discharge flat cell, copper cathode in argon).

and pressure at constant current is also more or less observed, although the length of the CDS seems to vary more rapidly than the pressure. In general, a satisfactory agreement between our calculated results and the empirical equation is found, which is considered as a validation of our present model.

Also, the energy distributions and mean energies of the plasma species can be calculated with the model. Fig. 9 shows the variation of the flux energy distribution of the electrons throughout the discharge (*i.e.*, at different positions from the cathode), at 1000 V, 75 Pa and about 3 mA. Electrons leave the cathode with low energies, but they gain energy from the electric field in the CDS. On the other hand, they also lose energy by collisions, so that their energy distribution is spread out over lower energies also. At the end of the CDS (*i.e.*, at 0.24 cm), a considerable fraction of the electrons has still not

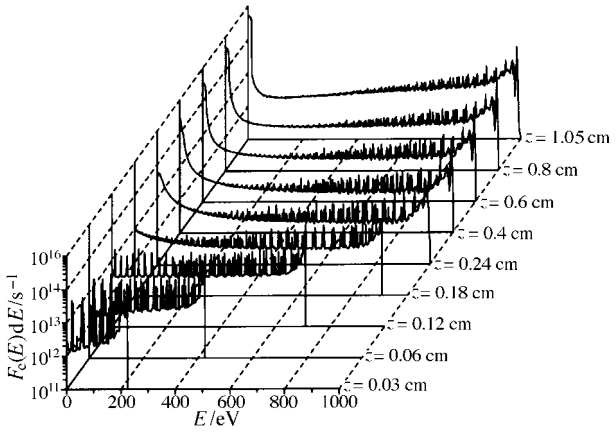

Fig. 9 Calculated flux energy distribution of the electrons, as a function of distance from the cathode (VG9000 glow discharge flat cell, 75 Pa, 1000 V, 3 mA, copper cathode in argon).

participated in any collision process in the CDS, as is indicated by the peak at the maximum attainable energy (1000 eV). In the NG, the electrons no longer gain much energy from the weak electric field, but they lose their energy by collisions. Therefore, the energy distribution changes shape: the low energy part grows, whereas the high energy part diminishes slightly.

The electron energy distribution in the NG seems to consist of three distinct electron populations: (i) the slow electron group with energies too low for inelastic collisions (*i.e.*, a few eV), (ii) the group of secondary electrons, which are emitted at the cathode but have lost energy by inelastic collisions, or which have been created in the glow discharge plasma (they possess energies still high enough for inelastic collisions, *i.e.*, ranging from several eV to slightly less than the full discharge voltage), and (iii) the primary electron group which are emitted from the cathode and have lost no energy by collisions (their energy is equal to the total voltage drop, *i.e.*, 1000 V). Under the present discharge conditions, about 50% of the electrons belong to the slow group. The secondary electron group comprises about 48% of the total electron population, and about 2% is found in the primary electron group, *i.e.*, those that have traversed the discharge without collisions.

Electron flux energy distributions have been measured with a retarding field analyzer in the NG of a helium glow discharge at a pressure of 10–15 Torr and a few hundred volts discharge voltage.[28] It was found that most electrons have, indeed, low energies, but a small peak is observed at maximum energy. Hence, the results are in good qualitative agreement with our calculations.

The spatial variation of the flux energy distribution of the argon ions, at 1000 V, 75 Pa and 3 mA, is presented in Fig. 10(*a*). The argon ions are assumed to be more or less thermalized in the NG, so that only the CDS is shown. The argon ions enter the CDS from the NG (in front of the figure, at $z = 0.24$ cm) and move towards the cathode ($z = 0$ cm, back of the figure), thereby gaining energy from the electric field and losing energy due to collisions. However, a peak at maximum energy, corresponding to ions that have lost no energy in collisions, is not observed, but the energy distribution decreases towards high energies. This indicates that the argon ions lose their energy much more efficiently by collisions than the electrons.

Flux energy distributions of the argon ions bombarding the cathode in a glow discharge cell of the VG9000 mass spectrometer have been measured by van Straaten *et al.*[29] The energy scans were recorded with the double-focusing mass spectrometer, by varying the acceleration voltage and keeping

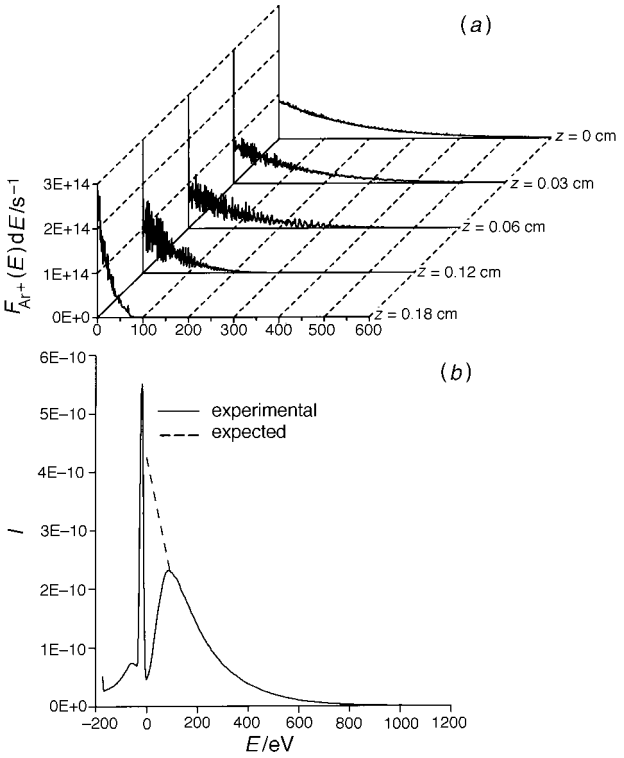

Fig. 10 (*a*) Calculated flux energy distribution of the argon ions in the CDS, as a function of distance from the cathode (VG9000 glow discharge flat cell, 75 Pa, 1000 V, 3 mA, copper cathode in argon). (*b*) Experimental flux energy distribution of the argon ions bombarding the cathode, measured with the VG9000 glow discharge mass spectrometer (at 1000 V, 3 mA, copper cathode in argon).

the magnetic field constant. The result at 1000 V and 3 mA is shown in Fig. 10(*b*). A dip in the distribution was observed at low energies. This was probably due to an experimental artefact. Indeed, a peak appeared at negative energy, and it was suggested that this peak corresponds to ions formed in the acceleration region outside the glow discharge cell, by symmetric charge transfer collisions of ions with low energy. The ions with low energy therefore disappear from the energy distribution, and this explains the dip at low energy. The broken line in Fig. 10(*b*) represents the expected energy distribution, which is in good agreement with the modeling result of Fig. 10(*a*).

Fig. 11 shows the spatial variation of the flux energy distribution of the fast argon atoms, at 1000 V, 75 Pa and 3 mA. Only the CDS is presented, since fast argon atoms exist only in this region. It should be borne in mind that the term 'fast

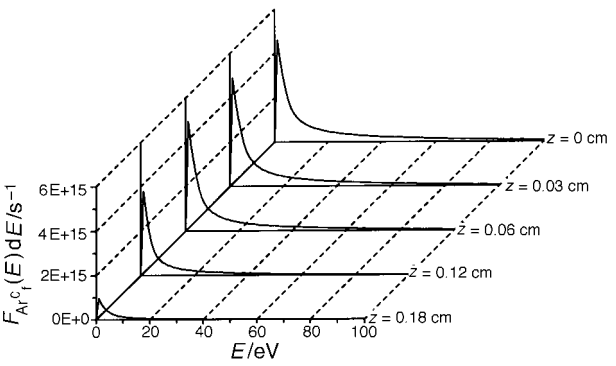

Fig. 11 Calculated flux energy distribution of the fast argon atoms in the CDS, as a function of distance from the cathode (VG9000 glow discharge flat cell, 75 Pa, 1000 V, 3 mA, copper cathode in argon).

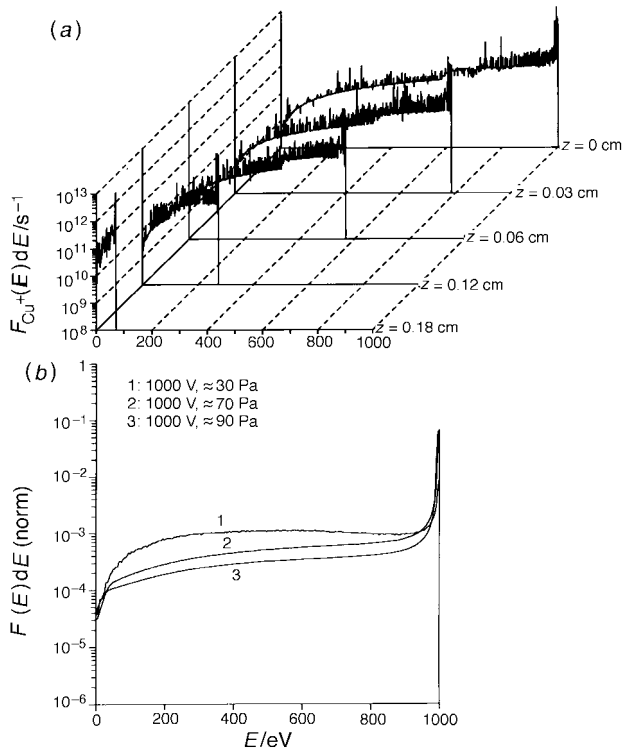

Fig. 12 (*a*) Calculated flux energy distribution of the copper ions in the CDS, as a function of distance from the cathode (VG9000 glow discharge flat cell, 75 Pa, 1000 V, 3 mA, copper cathode in argon). (*b*) Experimental flux energy distributions of the copper ions bombarding the cathode, measured with the VG9000 glow discharge mass spectrometer (at 1000 V, three pressures, copper cathode in argon).

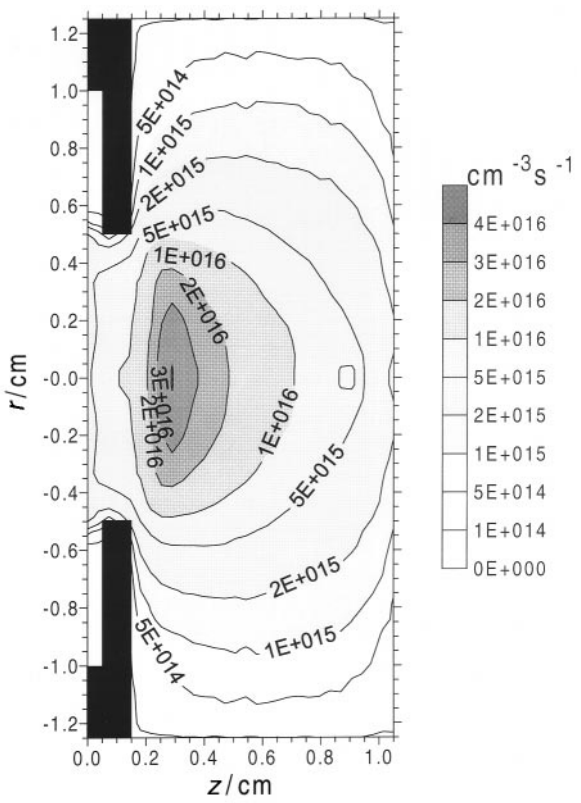

Fig. 13 Calculated electron impact excitation rate of argon ground state atoms throughout the discharge (VG9000 glow discharge flat cell, 75 Pa, 1000 V, 3 mA, copper cathode in argon).

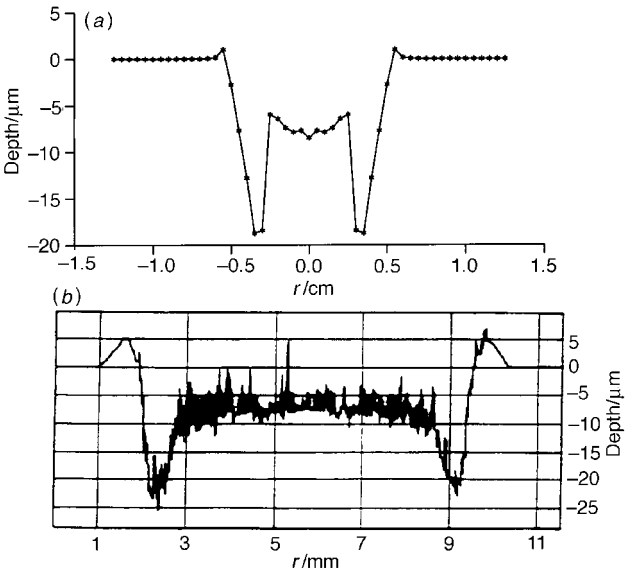

Fig. 14 (*a*) Calculated crater profile after 1 h of sputtering at the cathode (VG9000 glow discharge flat cell, 75 Pa, 1000 V, 3 mA, copper cathode in argon). Reprinted from ref. 30 with permission of Elsevier Science. (*b*) Experimental crater profile after 45 min of sputtering at the cathode, obtained with the VG9000 mass spectrometer (at 1000 V, 3 mA, copper cathode in argon).[31]

atoms' is used for those atoms with energies beyond 1 eV. Atoms with energies below 1 eV are assumed to belong to the thermalized group. This explains the dip in the distribution at 0 eV. Apart from that, the energy distribution resembles qualitatively that of the argon ions (*i.e.*, decreasing towards higher energies), which is obvious because the fast argon atoms are formed directly from the argon ions by symmetric charge transfer and elastic collisions. The energy distribution is, however, strongly shifted to lower energies compared with the argon ion energy distribution (note that the energy axis is truncated at 100 eV), because the atoms cannot gain energy from the electric field; they can only lose energy by collisions.

The flux energy distribution of copper ions (*i.e.*, copper was assumed as cathode) as a function of distance from the cathode, at 1000 V, 75 Pa and 3 mA, is depicted in Fig. 12(*a*). Only the CDS is shown, since the copper ions are thermalized in the NG. The copper ions start at the CDS–NG interface ($z =$ 0.24 cm, in front of the figure) with almost zero energy, and they gain energy on their way to the cathode. In contrast to the energy distribution of the argon ions, the energy distribution of the copper ions is characterized by a pronounced peak at the maximum possible energy (note the logarithmic scale). This indicates that most of the copper ions originate from the NG and pass the CDS without collisions.

The copper ion energy distribution has also been measured at the cathode, with the double-focusing VG9000 mass spectrometer.[29] The results are shown in Fig. 12(*b*). Since the pressure cannot generally be measured inside the glow discharge cell of the VG9000 instrument, three estimated pressure values are indicated for the three experimental energy distributions. The measured energy distributions are also characterized by a pronounced peak at maximum energy. Hence, reasonable agreement is reached between the experimental energy distribution and the modeling result of Fig. 12(*a*).

Since the Monte Carlo models describe the behavior of the plasma species explicitly, they can provide information about the individual collision processes incorporated in the model. Fig. 13 illustrates, for example, the electron impact excitation rate (from the ground state of argon atoms to all excited levels) throughout the discharge, at 1000 V, 75 Pa and 3 mA. The excitation is fairly low in the CDS and reaches a maximum at

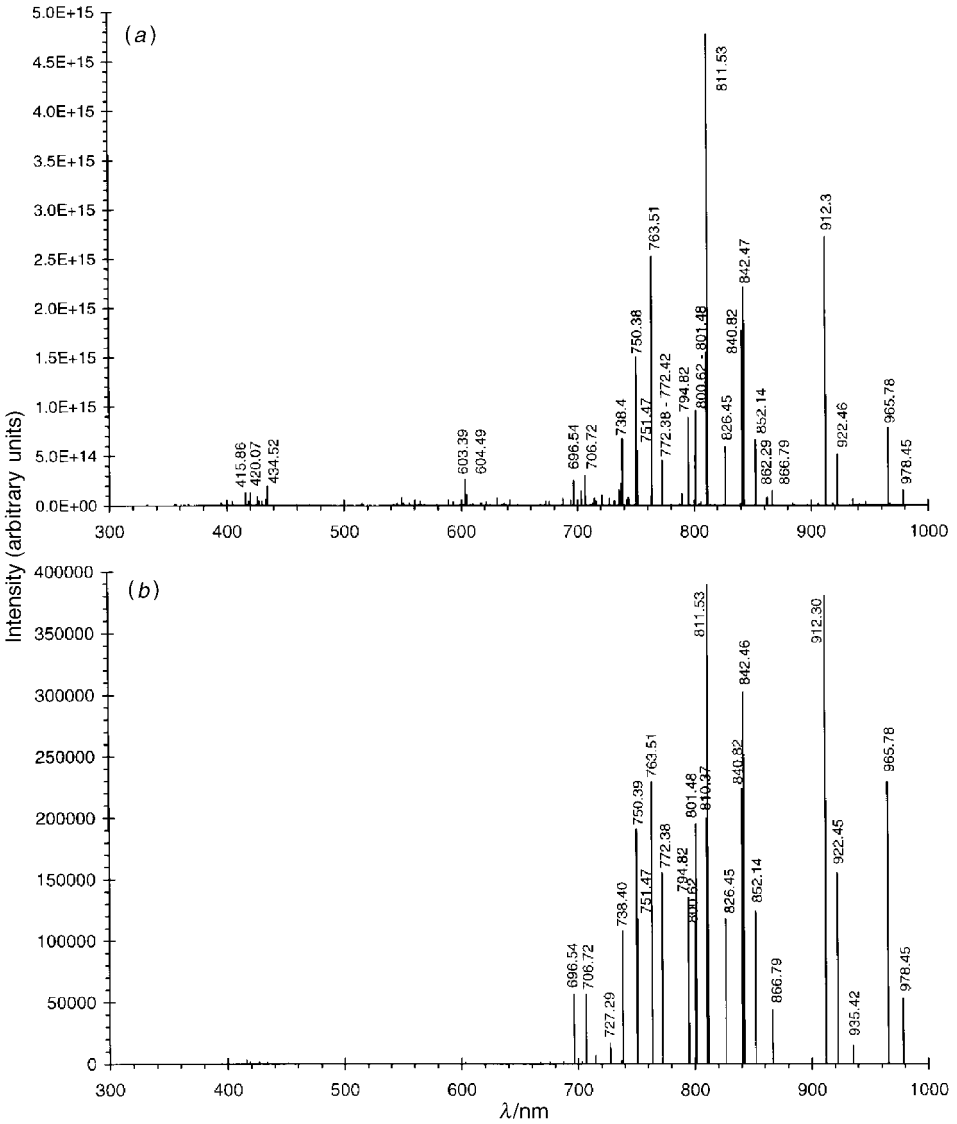

Fig. 15 (*a*) Calculated argon atomic optical emission spectrum at the beginning of the negative glow (at 0.17 cm from the cathode) (six-way cross glow discharge cell, 1000 V, 1 Torr, 2 mA, copper cathode in argon). (*b*) Experimental argon atomic optical emission spectrum, measured in a 60-cycle ac glow discharge at a current of 60 mA and a pressure of 3 Torr.[33] Reprinted from ref. 32 with permission of Elsevier Science.

the beginning of the NG, since the residence time of the electrons is highest there. This is in good agreement with visual observations of the glow discharge. Indeed, close to the cathode, the excitation is low, yielding also minor de-excitation and hence only weak emission of light. This corresponds to the dark region in front of the cathode, called therefore 'cathode *dark* space'. Further in the discharge, the excitation reaches a maximum, producing a large amount of de-excitation and hence strong emission of light. This gives rise to the bright region in the discharge, called 'negative *glow*'. It should be mentioned that, adjacent to the cathode, a very thin bright layer is often observed. This is attributed to argon ion and atom impact excitation, which reaches a maximum right at the cathode.[11]

Also, the collision rates of different ionization processes throughout the discharge can be calculated with the models, as was illustrated in refs. 9 and 10. For argon, it was found that electron impact ionization was most significant, although argon ion and atom impact ionization are not negligible. Integrated over the total discharge region, the relative contributions of these three processes amount to about 90, 2 and 8%, respectively, under both typical GDMS and GD-OES discharge conditions.[9,15] Stepwise electron impact ionization (*i.e.*, ionization from the argon metastable levels) and argon metastable atom–metastable atom collisions leading to the ionization of one of the atoms were found to be generally negligible. For the sputtered atoms, on the other hand, electron impact ionization was found to be of minor importance, whereas Penning ionization and also asymmetric charge transfer were found to play a dominant role. Integrated over the total discharge region, these three ionization processes have calculated contributions of the order of typically 2–4, 40–85 and 10–60%, respectively, depending on the discharge conditions (*i.e.*, Penning ionization is clearly dominant at low pressures, whereas asymmetric charge transfer gains importance at higher pressures), the cell geometry and the kind of cathode material.

In addition to making predictions about collision processes in the plasma, the models can also give more information about the sputtering process at the cathode, since fluxes and energy distributions of the bombarding species are known over the entire cathode surface. Fig. 14(*a*) presents a typical crater profile due to sputtering at the cathode, calculated at 1000 V, 75 Pa and 3 mA.[30] Fig. 14(*b*) illustrates an experimental crater profile measured under similar discharge conditions;[31] it can be seen that the calculated profile resembles qualitatively the

typical crater profiles found experimentally. Indeed, it is characterized by the crater edge effect (*i.e.*, the crater is much deeper at the sides than in the center), the non-steep crater walls and the small rim outside the crater profile. Moreover, the absolute values of the calculated crater depth are in reasonable agreement with the experimental values, which is a validation of the model.

Finally, from the collisional–radiative model, which describes the behavior of the various excited argon levels, we were also able to calculate the argon atomic optical emission spectrum in the glow discharge. Fig. 15(*a*) illustrates this calculated spectrum, at the beginning of the NG (*i.e.*, at about 0.15 cm from the cathode), for a six-way cross glow discharge cell at 1000 V, 1 Torr and 2 mA.[32] It can be seen that the lines in the region 700–1000 nm (*i.e.*, the so-called 'red lines', corresponding to 4p→4s transitions) clearly dominate the argon atomic spectrum. Fig. 15(*b*) depicts the argon atomic spectrum, found in the literature and measured in a 60 cycle ac glow discharge at 60 mA current and 3 Torr pressure.[33] In spite of the completely different discharge conditions, both spectra have a similar appearance (*i.e.*, the intensities of the various lines are comparable). This is not straightforward, in view of the large number of populating and depopulating processes taking place for the various levels, and the uncertainties in the cross-sections and transition probabilities needed for the model. Hence, the reasonable agreement between experiment and model shows that the latter presents a realistic picture of the glow discharge.

CONCLUSION

Typical results of our three-dimensional modeling work for a direct current glow discharge in argon are presented and compared with experimental observations to test the validity of the models. In general, satisfactory agreement has been reached, as was illustrated for the current–voltage characteristics, the density profiles of various plasma species, the flux energy distributions of ions bombarding the cathode, the crater profiles at the cathode and the argon atomic optical emission spectrum.

Exact quantitative agreement cannot yet be expected, since the input data used in the models (*e.g.*, cross-sections and rate coefficients of plasma processes, sticking coefficients at the walls) are subject to uncertainties, and a small error in the cross-sections can sometimes be amplified to fairly large uncertainties in the final calculations.[11] Also, the gas temperature in the plasma is not known exactly, and it is therefore used as a kind of fitting parameter to yield satisfactory agreement with experiment. The assumed value of 360 K seems reasonable, so that the models probably present a realistic picture of the glow discharge.

On the other hand, plasma diagnostic experiments are not always straightforward either. The glow discharge is confined to a small volume, which makes it difficult to perform accurate, spatially resolved, measurements. Also, one should be careful not to disturb the plasma too much in performing invasive experiments; this can be a problem in Langmuir probe measurements, for example. Furthermore, the measured values do not always give a correct picture of the actual quantities present in the plasma, and instrumental artefacts have to be accounted for, as was probably the case in our ion energy distribution measurements at the cathode. Moreover, it is difficult to carry out accurate absolute density measurements, as for example in laser-induced fluorescence spectroscopy, since transition probabilities, and other characteristic data required for calculating the results are subject to uncertainties, and the instruments have to be accurately calibrated, with respect to transmission, signal response, detection efficiency, *etc*. From these considerations it follows that the experimental results can also be subject to considerable uncertainties.

Therefore, we can conclude that modeling is a useful tool for obtaining better insight into the complexity of the glow discharge. It is complementary to experimental plasma diagnostics, since it can provide information that is experimentally hard to acquire.

A. B. is supported by the Fund for Scientific Research (FWO), Flanders. The authors also acknowledge financial support from the Federal Services for Scientific, Technical and Cultural Affairs (DWTC/SSTC) of the Prime Minister's Office through IUAP-IV (Conv. P4/10).

REFERENCES

1 Marcus, R. K., *Glow Discharge Spectroscopies*, Plenum Press, New York, 1993.
2 Payling, R., Jones, D., and Bengtson, A., *Glow Discharge Optical Emission Spectrometry*, Wiley, New York, 1997.
3 Bogaerts, A., van Straaten, M., and Gijbels, R., *Spectrochim. Acta, Part B*, 1995, **50**, 179.
4 Bogaerts, A., Gijbels, R., and Goedheer, W. J., *J. Appl. Phys.*, 1995, **78**, 2233.
5 Bogaerts, A., and Gijbels, R., *J. Appl. Phys.*, 1995, **78**, 6427.
6 Bogaerts, A., and Gijbels, R., *Phys. Rev. A*, 1995, **52**, 3743.
7 Bogaerts, A., van Straaten, M., and Gijbels, R., *J. Appl. Phys.*, 1995, **77**, 1868.
8 Bogaerts, A., and Gijbels, R., *J. Appl. Phys.*, 1996, **79**, 1279.
9 Bogaerts, A., Gijbels, R., and Goedheer, W. J., *Anal. Chem.*, 1996, **68**, 2296.
10 Bogaerts, A., and Gijbels, R., *Anal. Chem.*, 1996, **68**, 2676.
11 Bogaerts, A., PhD Dissertation, University of Antwerp, 1996.
12 Bogaerts, A., Gijbels, R., and Vlcek, J., *J. Appl. Phys.*, in the press.
13 Bogaerts, A., and Gijbels, R., *J. Anal. At. Spectrom.*, 1997, **12**, 751.
14 Bogaerts, A., and Gijbels, R., *J. Am. Soc. Mass Spectrom.*, 1997, **8**, 1021.
15 Bogaerts, A., and Gijbels, R., *Spectrochim. Acta, Part B*, in the press.
16 Bogaerts, A., and Gijbels, R., *Plasma Phys. Rep.*, in the press.
17 van Straaten, M., unpublished work.
18 Ferreira, N. P., Human, H. G. C., and Butler L. R. P., *Spectrochim. Acta, Part B*, 1980, **35**, 287.
19 Fang, D., and Marcus, R. K., *Spectrochim. Acta, Part B*, 1990, **45**, 1053.
20 Fang, D., and Marcus, R. K., *Spectrochim. Acta, Part B*, 1991, **46**, 983.
21 Büger, P. A., *Z. Naturforsch.*, 1975, **30**, 216.
22 Kuraica, M., Konjevic, N., Platisa, M., and Pantelic, D., *Spectrochim. Acta, Part B*, 1992, **47**, 1173.
23 Bogaerts, A., Quentmeier, A., Jakubowski, N., and Gijbels, R., *Spectrochim. Acta, Part B*, 1995, **50**, 1337.
24 Bogaerts, A., Guenard, R. D., Smith, B. W., Winefordner, J. D., Harrison, W. W., and Gijbels, R., *Spectrochim. Acta, Part B*, 1997, **52**, 219.
25 Strauss, J. A., Ferreira, N. P., and Human, H. G. C., Spectrochim. Actam Part B, 1982, 37, 947.
26 Bogaerts, A., Wagner, E., Smith, B. W., Winefordner, J. D., Pollmann, D., Harrison, W. W., and Gijbels, R., *Spectrochim. Acta, Part B*, 1997, **52**, 205.
27 Aston, F. W., *Proc. R. Soc. London, Ser. A*, 1907, **78**, 80.
28 Gill, P., and Webb, C. E., *J. Phys. D: Appl. Phys.*, 1977, **10**, 299.
29 van Straaten, M., Bogaerts, A., and Gijbels, R., *Spectrochim. Acta, Part B*, 1995, **50**, 583.
30 Bogaerts, A., and Gijbels, R., *Spectrochim. Acta, Part B*, 1997, **52**, 765.
31 Jonkers, C., PhD Dissertation, University of Antwerp, 1995.
32 Bogaerts, A., Gijbels, R, and Vlcek, J., *Spectrochim. Acta, Part B,* in the press.
33 Gray, D. E., *American Institute of Physics Handbook*, McGraw-Hill, New York, 3rd edn., 1972.

Paper 8/00329G
Received January 12, 1998
Accepted February 28, 1998